Research Article

Yang Wang, Dan Lei, Liangke Wu*, Ning Hu, Huiming Ning*, Alamusi, and Yaolu Liu

Preparation of PVDF-HFP/CB/Ni nanocomposite films for piezoelectric energy harvesting

https://doi.org/10.1515/rams-2023-0146
received March 04, 2023; accepted October 25, 2023

Abstract: As a representative flexible piezoelectric polymer, polyvinylidene fluoride (PVDF) and its copolymers have been widely used in energy harvesters and piezoelectric sensors. In this work, hybrid nanocomposite films were prepared by adding a small amount of carbon black (CB) and Ni nanoparticles to the poly(vinylidene fluoride-*co*-hexafluoropropylene) (PVDF-HFP) matrix using the solution casting method, followed by stretching and poling to increase the electroactive β-phase content. The results show that the hybrid fillers consisting of 0.3 wt% CB and 0.1 wt% Ni nanoparticles exhibit the best piezoelectric performance. The maximum output voltage of the PVDF-HFP/CB/Ni films reaches 3.5 V under 1 mm micro-vibration, which is 75% higher than that of pure PVDF-HFP films. Characterization results by X-ray diffraction analysis, Fourier-transform infrared spectrometry, and differential scanning calorimeter analysis show that the hybrid fillers are more effective in promoting the phase transformation from the α-phase to the β-phase in the matrix due to synergistic effect.

Keywords: PVDF-HFP, Ni nanoparticle, carbon black, piezoelectricity, synergistic effect

*** Corresponding author: Liangke Wu,** College of Aerospace Engineering, Chongqing University, Chongqing 400044, China, e-mail: wuliangke@cqu.edu.cn, tel: +86-02365102510
*** Corresponding author: Huiming Ning,** College of Aerospace Engineering, Chongqing University, Chongqing 400044, China, e-mail: ninghuiming@cqu.edu.cn, tel: +86-02365102510
Yang Wang, **Yaolu Liu:** College of Aerospace Engineering, Chongqing University, Chongqing 400044, China
Dan Lei: AECC Guizhou Honglin Aero-engine Control Technology Co., Ltd, Guiyang 550025, China
Ning Hu: College of Aerospace Engineering, Chongqing University, Chongqing 400044, China; State Key Laboratory of Reliability and Intelligence Electrical Equipment, School of Mechanical Engineering, Hebei University of Technology, Tianjin 300401, China
Alamusi: State Key Laboratory of Reliability and Intelligence Electrical Equipment, School of Mechanical Engineering, Hebei University of Technology, Tianjin 300401, China

1 Introduction

Piezoelectric energy harvesters can convert low-frequency mechanical energy from the environment into electrical energy to enable self-powered micro-devices [1]. Compared with traditional piezoelectric ceramics, polyvinylidene fluoride (PVDF) and its copolymers offer numerous advantages such as high flexibility, substantial piezoelectricity, and high ductility, which make them highly suitable for applications that require large bending and twisting capabilities [2–4]. Therefore, nanocomposites based on PVDF and its copolymers are considered ideal materials for manufacturing flexible piezoelectric energy harvesters. PVDF is a semi-crystalline polymer that possesses at least five polymorphs, *i.e.*, *α*, *β*, *γ*, *δ*, and *ε*. Among these, the α-phase has the semi-trans (TGTG′) conformation that is non-polar and exhibits no piezoelectricity, while the β-phase has the all-trans (TTTT) conformation that is highly polar and contributes the most to piezoelectric performance. However, solution-processed pristine PVDF thin films are non-ferroelectric because the most thermodynamically stable (majority) polymorph is the non-polar α-phase [5,6]. Therefore, increasing the content of the piezoelectric β-phase of PVDF has become a major focus of research at this stage. In recent decades, various processes have been developed to increase the content of the β-phases, such as mechanical stretching [7,8], annealing treatment [9], and high electric field poling [10]. Among these methods, mechanical stretching is the most commonly used approach for transforming the α-phase to the β-phase. During the stretching process, the applied stress to the film results in the re-alignment of polymer chains into a fiber-like structure, by which the all-trans (TTTT) conformation is induced. Additionally, stretching forces the dipoles of the polymer chains to align normally to the stretching direction [7,11]. Furthermore, many studies have found that the introduction of nanofillers (such as graphene [12–14], carbon nanotubes [15,16], and CB [carbon black] [17]) can alter the crystal structure of the matrix, thereby enhancing the piezoelectricity. Wu *et al.* incorporated graphene into PVDF-trifluoroethylene (TrFE) by the solution casting method to prepare piezoelectric nanocomposite films. The PVDF-TrFE/graphene (0.15 wt%)

film generated a calibrated open-circuit voltage of 12.43 V, which was 104% higher than that of pure PVDF-TrFE films and the harvested power density was increased by 302% (AC circuit) and 359% (DC circuit), respectively [18]. Gan and Majid prepared PVDF/TiO_2 composite films and observed that the DC conductivity of the polymer matrix was increased, greatly lowering the requirement of the poling electric field (decreasing from 260 to 120 MV·m^{-1}) [19]. Recently, Lei *et al.* incorporated Ni nanofillers into the poly(vinylidene fluoride-*co*-hexafluoropropylene) (PVDF-HFP) matrix and applied high voltage poling (E_{max} = 130 MV·m^{-1}), by which the relative fraction of the β-phase increased to 98%, and the calibrated open-circuit voltage reached 3.84 V [10].

In general, the mechanisms for enhancing phase transformation by nanofillers mainly include inherent piezoelectric properties, nucleating effect and interface coupling effect [20]. However, due to the different interfaces between nanofillers and PVDF matrix, there are still some challenges that need to be overcome to completely understand the mechanism. For example, the van der Waals force between fillers can lead to uneven distribution and agglomeration of the nanofillers, which requires further chemical or physical modification of the nanofillers [21,22]. Besides, high-conductive fillers are usually more likely to cause breakdown failure during poling [23,24], while poor conductive nanofillers limit their piezoelectric properties to some extent [25].

The efficacy of hybrid nanofillers has been confirmed by a large number of studies [26–28]. Cai *et al.* prepared PVDF-HFP/CB/GO composite films and found that the hybrid fillers could effectively promote the phase transition in the initial stage of crystallization. As a result, the films can reach a higher β-phase fraction at a lower concentration, and the maximum output voltage and collected power density are 181 and 329% of the neat PVDF-HFP films, respectively [29]. Similarly, Khalifa *et al.* added ZnO-modified single-walled carbon nanotubes (SWCNT) to PVDF to prepare piezoelectric films with high power generation capabilities. The synergistic effect between the hybrid fillers results in the adsorption of the TTTT chains on the surfaces of the carbon nanotubes (CNT), leading to highly ordered β-crystals with significantly increased generated voltage [30]. Additionally, GO-Ag nanocomposites have been reported to exhibit different piezoelectric properties under lighting and blackout conditions due to the interaction of PVDF matrix, Ag nanoparticles, and GO nanoparticles [31]. The highly conductive CB has also shown a significant effect on the piezoelectricity of PVDF-HFP due to its abundant functional groups on its surface, which is beneficial for good dispersion in polar solvents [29,32,33]. Similarly, modified Ni nanoparticles, which possess hydroxyl groups on their surfaces, can induce the formation of the polar phase of PVDF-HFP [10,34,35]. Therefore, in this work, these two nanofillers were selected to improve the piezoelectricity of the composite films. The comparison of the performance of the PVDF-HFP composite films in our previous works [10,25,29,36,37] is given in Table 1. For other research groups, due to the differences in the preparation methods and measurement conditions, the results are quite different from each other, as shown in Table 2 [38–44].

In recent years, hybrid nanofillers have been used as nucleating agents to further improve phase transformation based on their synergistic effects. In this study, PVDF-HFP/CB/Ni composite piezoelectric films were prepared by the solution casting method. By adjusting the ratio of CB and Ni nanoparticles in the composite, we aimed to explore the effect of CB/Ni hybrid fillers on the initial crystallization, stretching, and poling processes of the films.

2 Experimental

2.1 Materials

Compared to PVDF, PVDF-HFP has the advantages such as better flexibility, lower cost, and higher pyroelectric coefficient. In this work, PVDF-HFP was utilized as the piezoelectric matrix.

Table 1: Comparison of research on piezoelectric properties of PVDF–HFP with various processes of poling

Material	Poling electric field (MV·m^{-1})	Calibrated open-circuit voltage (V)	Ref.
PVDF-HFP/Ni	130	3.84	[10]
PVDF-HFP/rGO	90	3.56	[36]
PVDF-HFP/AgNW	70	2.14	[37]
PVDF-HFP/VGCF	60	1.25	[25]
PVDF-HFP/MWCNT	60	1.35	[25]
PVDF-HFP/CB/FLG	90	4.14	[29]
PVDFHFP/CB/Ni	120	4.17	This work

Table 2: Comparison of the power capability of PVDF and its copolymer-based composites

Material	Output voltage (V_{p-p})	Power density ($W \cdot m^{-3}$)	Remarks	Ref.
PVDF/Al_2O_3-rGO	36	28.0	Poling free	[38]
PVDF	6	0.48	Electrospun	[39]
PVDF/rGO	16	28	Electrospun	[40]
PVDF/$CsPbBr_3$/$Ti_3C_2T_x$	300	0.36	Self-polarization	[41]
PVDF-HFP/$NiFe_2O_4$	5	—	Electrospun	[42]
PVDF/$NaNbO_3$/rGO	2.16	—	Poling free	[43]
PVDF/Y-ZnO	25	36	Corona poling	[44]

PVDF-HFP was purchased from Arkema Inc. Its melting temperature is 140–145°C, and the melt flow rate (232°C, 125 kg) is 0.35–0.75 $g \cdot min^{-1}$. Dimethylformamide (DMF) was provided by Shanghai Titan Scientific Co. Ltd., spherical Ni nanoparticles (purity: 99.9%; size: 20–100 nm) were purchased from XF NANO Inc., and CB (size: 30–45 nm, specific surface area: 120–130 $m^2 \cdot g^{-1}$) was purchased from Macklin Inc. scanning electron microscopy (SEM) images of Ni and CB nanoparticles are shown in Figure 1. The Fourier-transform infrared (FTIR) spectrum of Ni nanoparticles is shown in Figure 2. The characteristic peak at 543 cm^{-1} corresponds to Ni nanoparticles, while the characteristic peak near 3,424 cm^{-1} corresponds to the stretching vibration of hydroxyl (–OH) groups on the surface of Ni nanoparticles. Some published studies have shown that hydroxyl groups can effectively improve the dispersion of nanoparticles in the PVDF-HFP matrix due to the interaction between the molecular chains and the hydroxyl groups, thus inducing the formation of β-phases [10]. All materials were used as received.

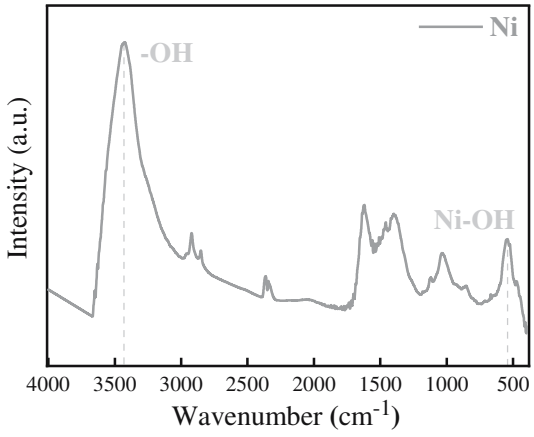

Figure 2: FT-IR spectrum of Ni nanoparticles.

2.2 Preparation of PVDF-HFP/CB/Ni nanocomposite films

PVDF-HFP films usually require stretching and poling to generate piezoelectric properties. Among the fabrication methods of PVDF films, electrospinning is an effective method that carries both stretching and poling simultaneously. However, the cost is higher, and it is obviously affected by the environmental and operating conditions, resulting in an unstable output. The simultaneous stretching and poling were also reported by other researchers [45,46]. Mahadeva *et al.* applied sequential stretching and corona poling to fabricate piezoelectric PVDF thin films and investigated the effects of poling time and grid voltage on the phase transformation and piezoelectricity. It was found that the poling time and the grid have no substantial

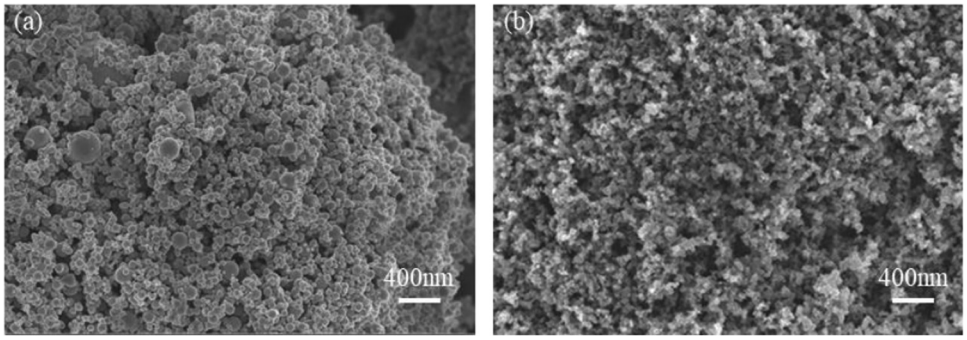

Figure 1: SEM images of nanofillers: (a) Ni and (b) CB.

influences on the phase transformation, indicating that the phase transformation mainly occurs during the stretching process. However, the poling has decisive effects on the piezoelectricity because of its function in dipole moment alignment [45]. The simultaneous stretching and poling were also developed in the 3D printing technique in recent years. Lee and Tarbutton developed an innovative method to print PVDF filament rods under a strong electric field in which poling and stretching can be carried out simultaneously. A high electric field is applied to the molten polymer column between the nozzle tip and the printing bed (poling) during extrusion (stretching), which leads to the molecular chain alignment and the phase transformation to β-phase [46]. The solution casting method is used to prepare films by separating uniaxial stretching and poling. Although the process is relatively cumbersome, the operation is simple and suitable for large-scale industrial production. Therefore, the solution casting method is utilized to prepare initial crystalline films in this work. The preparation process of PVDF-HFP-based composite films is similar to that previously reported [17,25] (Figure 3), and can be described briefly as follows: (a) The determined mass of CB and Ni nanoparticles (calculated by the nanofiller content in the matrix) is added into 24 g of DMF, then ultra-sonication is applied for 5 min to achieve uniform dispersion, and then 8 g of the PVDF-HFP powder is added into the DMF/CB/Ni suspension by planetary stirring, ultrasonic stirring and mechanical defoaming in sequence. (b) The mixed solution is poured onto an Al plate (thickness: 1 mm) and heated to 90°C for 2 h for initial crystallization. (c) Uniaxial thermal stretching (60°C) is applied on the films at a tensile rate of 10 mm·min^{-1} and an elongation ratio of 4.5–5. The thicknesses of the films prepared range from 250 to 270 μm. During the uniaxial stretching process, the film and fixture will experience relative sliding, when the stretching stroke is set to 100 mm, the elongation of the film can be maintained at 4.5–5. (d) The films are cut into sizes of 2.5 cm × 3 cm (in the stretching direction), and two Al foils are pasted on both sides of the films by conductive epoxy adhesive (ITW Chemtronics CW2400). (e) Poling in silicone oil is applied by a step-wise method. The initial electric field is 10 MV·m^{-1}, the increment for each step is 10 MV·m^{-1} and the maximum electric field is 120 MV·m^{-1}. The schematic of the step-wise poling method is shown in Figure 4. The photo of the poling process is shown in the Supplementary information.

For simplicity, the samples are named by the nanofiller content. For example, C0.3N0.1 represents a sample containing 0.3 wt% CB and 0.1 wt% Ni nanoparticles. In this work, the maximum poling electric field of pure PVDF-HFP, C0.3, and C0.5 films is 100 MV·m^{-1}, and the maximum poling electric field of C0N0.1, C0.5N0.1, and C0.3N0.1 is 120 MV·m^{-1}.

2.3 Electrical experiments

The structure of the test plate and the measurement mechanism of the generated output voltage are shown in

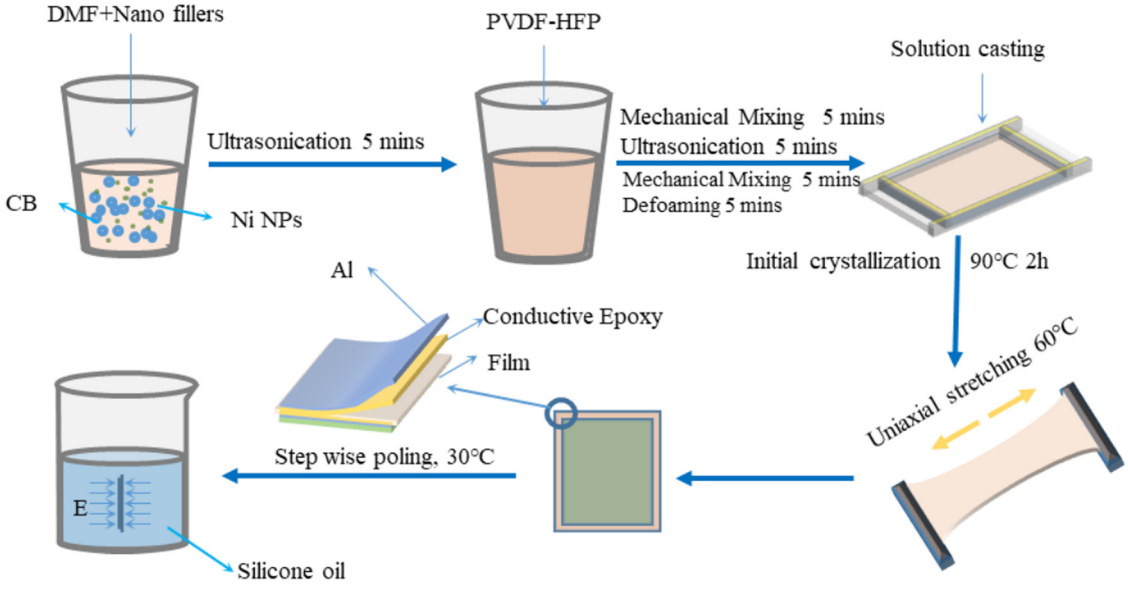

Figure 3: The preparation process of PVDF-HFP/CB/Ni composite films.

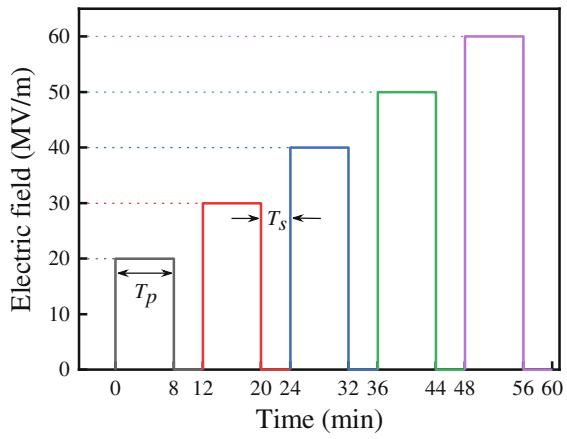

Figure 4: Schematic of the electric field during the step-wise poling (T_p: poling time; T_s: pause time).

Figure 5. In the experiment, a copper foil electrode is drawn from one side of the piezoelectric film. Different from previous reports, in this work, we encapsulated the prepared films by PI films to avoid bubbles between the epoxy resin (adhesive) and the piezoelectric film. Three pieces of piezoelectric films with the same component were glued by epoxy resin on the Al plate with wires connected for the measurement of the output voltage. The measurement mechanism of the generated voltage is shown in Figure 5(b). The equipment involved in the test includes a signal generator (AFG3022), a power amplifier (HAS0112), a displacement sensor (CD5-125/LW25), and an oscilloscope (TDS3034B). The testing process is as follows. At first, a magnet is attached to the underside of the Al plate; then, the electromagnet under the magnet is excited by a sinusoidal signal (f: 25–27 Hz) to induce harmonious vibration of the Al plate, which in turn produces a periodical strain on the piezoelectric film. Under the excitation of a magnetic field, the film generates a periodical voltage. Finally, the generated voltage is recorded with an oscilloscope [17]. Due to the periodic sinusoidal vibration of the aluminum plate, the root mean square of the output voltage can be directly read from the oscilloscope, which is called the effective output voltage of the film.

2.4 Characterization of PVDF-HFP/CB/Ni composite films

A field emission SEM (SEM TM4000 Plus II) was used to observe the cross-sectional morphologies of the samples. Before observation, the sample surface was sputter-coated with gold using a magnetron.

An FTIR spectrometer (FTIR Nicolet IS50) was used to characterize the crystal structure of the polymers. The relative fraction of the β-phase ($F(\beta)$) in the composite films is calculated by the following formula:

$$F(\beta) = \frac{A_\beta}{\left(\frac{k_\beta}{k_\alpha}\right)A_\alpha + A_\beta} = \frac{A_\beta}{1.26A_\alpha + A_\beta}, \quad (1)$$

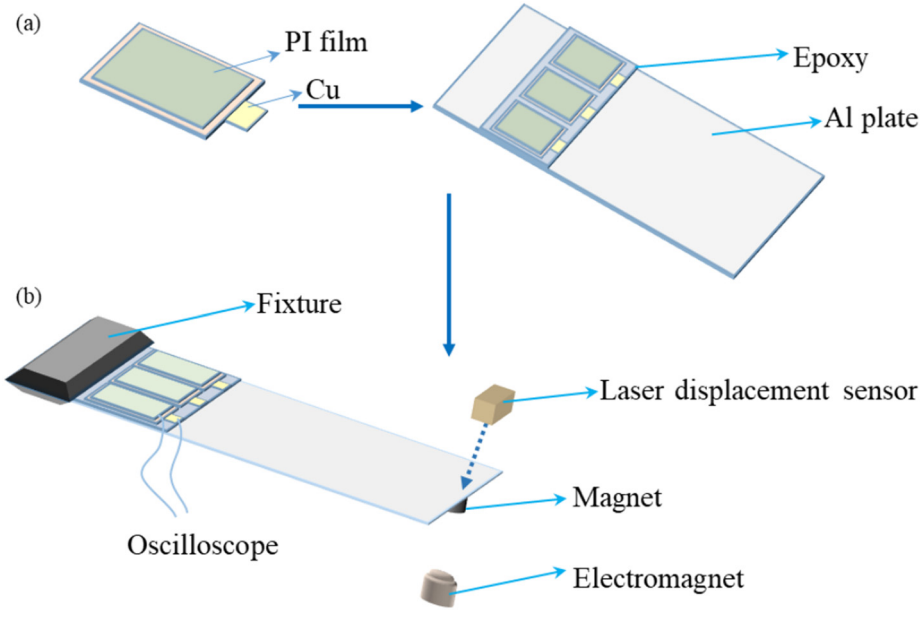

Figure 5: The measurement mechanism of the generated output voltage. (a) The preparation of the vibration plate; (b) Schematic of the measurement setup.

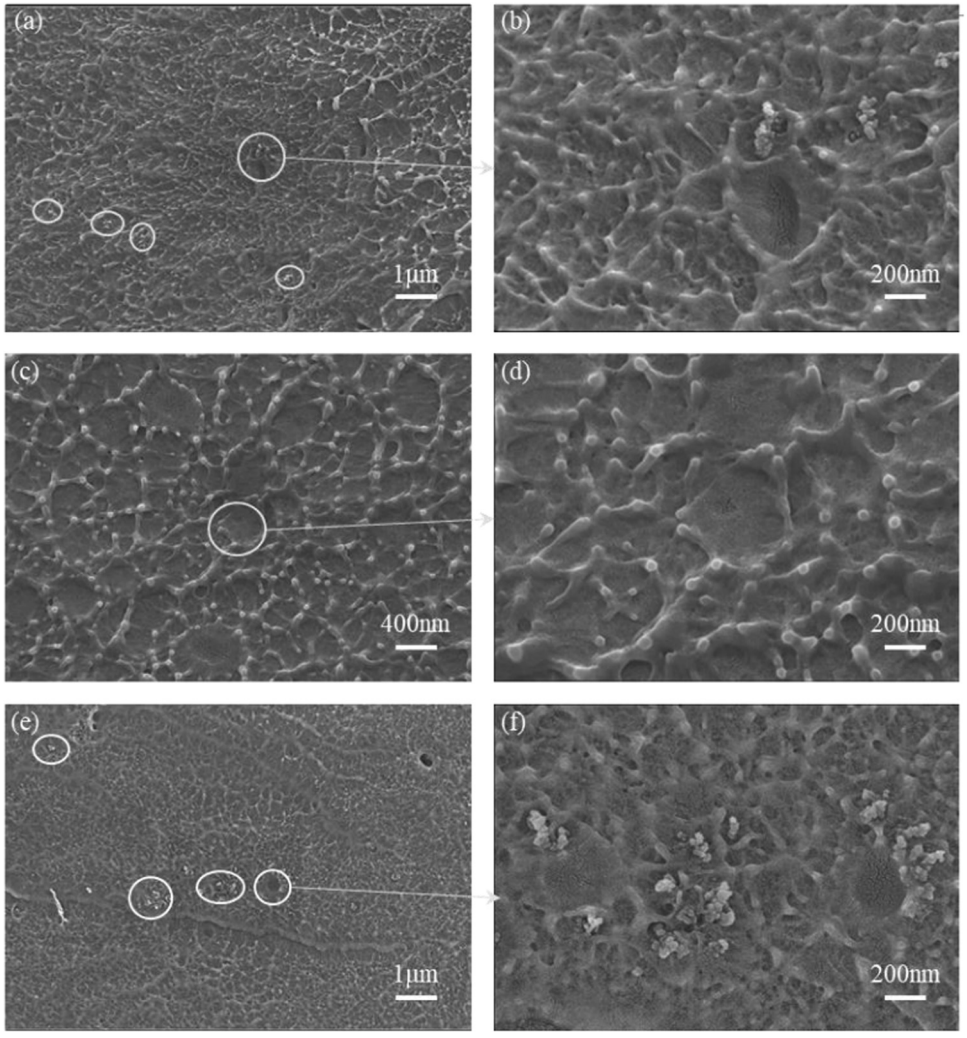

Figure 6: Cross-sectional SEM images of PVDF-HFP/CB/Ni composite films (initial crystallization): (a) C0.3, (b) C0.3 (high magnification), (c) N0.1, (d) N0.1 (high magnification), (e) C0.3N0.1, and (f) C0.3N0.1 (high magnification).

where A_α and A_β represent the absorbances at 765 and 840 cm^{-1}, respectively [47,48].

X-ray diffraction (XRD; X'Pert Powder) was used to characterize the structure of the piezoelectric composite films, which was operated at 40 kV and 40 mA with CuKα (λ = 1.5418 Å).

Differential scanning calorimeter (DSC; DSC3+) was used to investigate the crystallization degree and melting behavior of the samples. The measurements were conducted from 40 to 200°C at heating and cooling rates of 10°C·min^{-1}. The crystallinity degree X_c of the PVDF-HFP films can be calculated by the following formula:

$$X_c = \left(\frac{\Delta H_m}{\Delta H_m^\Phi}\right) \times 100\%, \quad (2)$$

where ΔH_m is the melting enthalpy of the composite material shown by the calculation software, and ΔH_m^Φ is the enthalpy of 100% crystalline PVDF-HFP material, *i.e.*, 104.5 J·g^{-1} [48].

In order to verify that the mechanism of the output voltage is piezoelectricity, the PVDF-HFP/C0.3N0.1 composite film is characterized by a piezoelectric force microscope (PFM; Bruker Icon). In the test, the PFM works in the contact mode, and the scanning area is 10 μm × 10 μm. The bias voltage is from −10 to 10 V, and the scanning frequency is 1 Hz.

In this study, "U", "S," and "P" represent samples in three stages: initial crystallization film (unstretched), after stretching (stretched), and after stretching and polarization (poled), respectively.

3 Results and discussion

3.1 Structure and morphology of PVDF-HFP/CB/Ni composite films

Figure 6 shows the SEM images of the cross-section of the initial crystallization films. The distribution of the nanofillers in the polymer matrix is a critical factor in determining the piezoelectric properties of the film [49]. Figure 6(a) and (b) shows the morphology of the C0.3 composite film. It can be seen that the CB particles are agglomerated within the matrix. In contrast, Figure 6(c) and (d) depicts the morphology of the composite film N0.1, which demonstrates that Ni nanoparticles exhibit good compatibility with the matrix, and almost no agglomeration is observed. Previous studies have suggested that the surface of Ni nanoparticles contains –OH groups that have a large specific surface area and a large coverage area, leading to good compatibility with the PVDF matrix [10]. Figure 6(e) and (f) presents the morphology of the film C0.3N0.1, and it is apparent that the hybrid nanofillers form weaker agglomerations compared to the mono-filler. The agglomeration may affect the synergistic effect to some extent.

3.2 Phase transformation of PVDF-HFP/CB/Ni composite films

3.2.1 XRD

Figure 7 depicts the XRD pattern of the composite films at three stages with marked characteristic peaks corresponding to α- and β-phases [9]. Figure 7(a) shows that the initial crystallization of pure PVDF-HFP film is predominantly in the α-phase, as evidenced by the clear characteristic peaks of the α-phase. However, in the composite films, the characteristic peaks of the α-phase nearly disappear, indicating a phase transformation from α-phase to β-phase after the addition of nanofillers. Figure 7(b) and (c) shows the spectra of the stretched films and polarized films, respectively. Strong

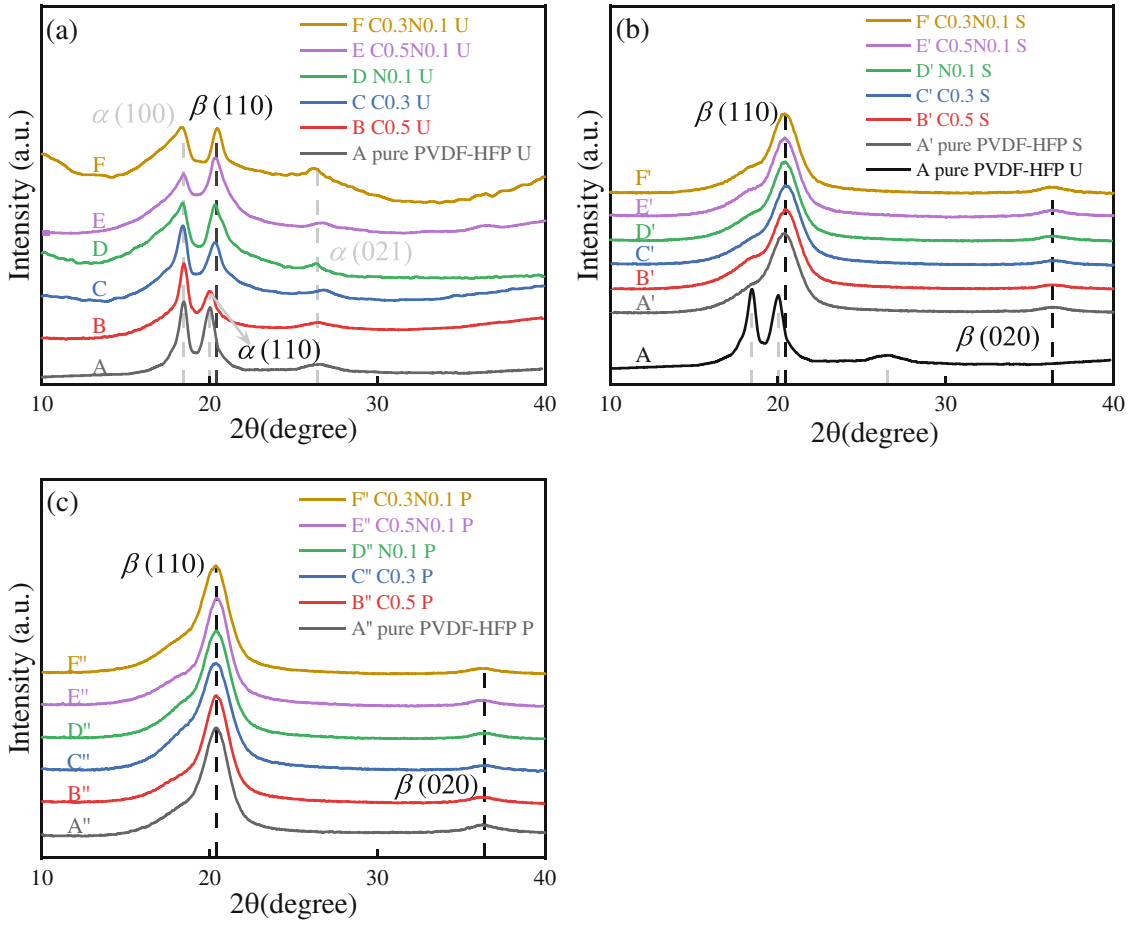

Figure 7: XRD spectra of PVDF-HFP/CB/Ni composite films: (a) unstretched films, (b) stretched films, and (c) stretched plus polarized films.

β-phase characteristic peaks are observed in all spectra, indicating that stretching can effectively increase the fraction of the polar β-phase. In order to further analyze the function of nanofiller addition, the relative fraction of the β-phase $F(\beta)$ is calculated from the FT-IR spectra.

3.2.2 FT-IR

FT-IR spectra of the composite films in the wavenumber range from 1,000 to 600 cm^{-1} are shown in Figure 8. The peaks at 615, 765, 795, and 975 cm^{-1} correspond to the α-phase, and the peaks at 840 cm^{-1} correspond to the β-phase [47]. In pure PVDF-HFP films, the α-phase dominates. However, with the addition of CB/Ni hybrid fillers, the α-phase characteristic peaks are significantly weakened, while the β-phase characteristic peaks become more obvious. The spectra of both stretched films and stretched + poled films (Figure 8(b) and (c)) show that the α-phase characteristic peaks almost disappear, indicating the phase transformation is fully completed during the stretching process.

In order to gain further insight into the mechanism underlying the enhancement of piezoelectric performance in polymer films by hybrid fillers, the relative fraction of the β-phase $F(\beta)$ at each stage of the composites was calculated by Eq. (1) and is presented in Figure 8(d). The results show that while the α-phase dominates, a small amount of the β-phase is present in the unstretched pure PVDF-HFP films, owing to the formation of β-phase molecular chains induced by the polar solvent DMF. For films containing CB or Ni nanoparticles, CB or Ni nanoparticles have a large specific surface area, which can affect the orientation and arrangement of matrix molecular chains, promoting the formation of β-phase. Therefore, $F(\beta)$ increases primarily due to the nucleate function of nanofillers. In the composites containing both nanofillers, the synergistic effect can combine the advantages of both nanofillers to promote the formation of β-phase and the crystallinity degree [10,24]. Compared to the composite film with CB and Ni added separately, the introduction of mixed fillers has a more complex effect on the films, as shown in Figure 8(d). For the initial crystalline films, the $F(\beta)$ of the composite films

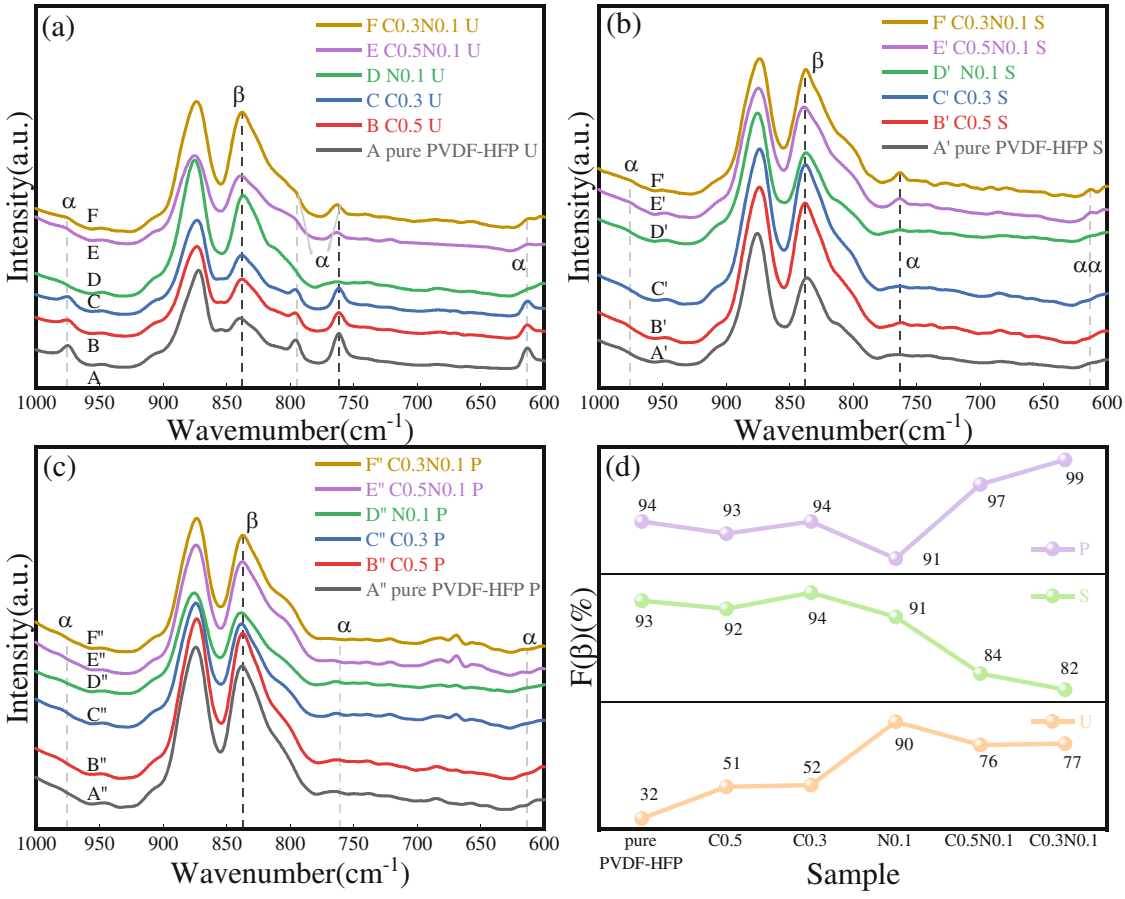

Figure 8: FT-IR spectra of PVDF-HFP/CB/Ni composite films: (a) unstretched films; (b) stretched films; and (c) stretched and polarized films. (d) The relative fraction of the β-phase $F(\beta)$ of the composite film at each stage.

containing 0.3 and 0.5 wt% CB increased to over 50%, higher than that of pure film. When CB is co-doped with 0.1 wt% Ni, $F(\beta)$ reached over 75%, reflecting the impact of hybrid fillers on the promoting effect of β-phase formation. It is worth mentioning that in films containing 0.1 wt% Ni (PVDF-HFP/N0.1), $F(\beta)$ reached 90%, higher than the PVDF-HFP/CB/Ni film. The SEM characterization results indicate that this may be caused by the inevitable aggregation of mixed fillers, but overall, the $F(\beta)$ of the hybrid filler film was significantly higher than pure films.

For the unstretched samples, the crystal region is dominated by the α-phase (spherical structure). During the stretching process, the applied stress (concentrated on the interface between the nanofillers and the matrix) forces the spherical structure to form a fiber-like structure, which is beneficial for the formation of zigzag conformation (TTTT, corresponding to β-phase) [50]. Poling is a necessary condition for obtaining piezoelectric properties of piezoelectric films. The added nanofillers can form micro-capacitors to induce a strong local electric field, which can improve the effect of poling [51].

In the stretched films and stretched + poled films, $F(\beta)$ increased dramatically, compared to the unstretched films. It is worth mentioning that in PVDF-HFP/CB/Ni hybrid films, the tensile process has a minimal effect on the transformation from the α-phase to the β-phase. In contrast, poling can significantly increase $F(\beta)$, probably due to the negative effect of hybrid filler aggregation during the stretching process [52,53].

In summary, the enhancement mechanism of PVDF phase transition at each stage can be summarized as follows. (a) The added nanofillers act as nucleation agents during the initial crystallization of PVDF-HFP, thereby increasing the crystallization rate and promoting the formation of β-phase. (b) During the stretching process, the stress concentration on the surfaces between the nanofillers and the matrix forces the elongation of the molecular chains, which is beneficial for the transformation from the α-phase to the β-phase. (c) The energy provided by the polarization process promotes the full conversion of a portion of the α-phase to the β-phase, thereby further increasing the $F(\beta)$. This study demonstrates that CB and Ni nanoparticles have a synergistic effect on promoting the formation of β-phases, resulting in increased output voltage compared with monoparticle systems.

3.2.3 DSC

Figure 9(a)–(c) shows the DSC thermograms of the nanocomposite films at each stage, where T_m represents the melting temperature of the material. After the addition of the nanofillers, the melting temperature of the composite shows a decrement trend due to the change in crystallinity and crystal structure. Figure 9(d) shows the crystallinity degree X_c of the composite film at each stage, calculated by Eq. (2). In general, the crystallinity degrees in all films are close to 40%. In the initial crystallization films, the crystallinity degree of the hybrid film decreases slightly, which may be caused by multiple factors, such as the size, distribution, and curvature of the additive [33]. For the stretched and poled films, the crystallinity degree is slightly increased. Although the process of stretching and poling induces molecular chain re-orientation and the formation of a new crystalline region, these processes also amplify defects within the material. As a result, it is challenging to predict the exact evolution of crystallinity change.

3.2.4 PFM

Figure 10 shows the PFM images of stretched and poled PVDF-HFP/CB/Ni composite films. With the applied AC bias between the PFM tip and bottom electrodes, the piezoelectric response of the films led to the deflection in the PFM cantilever at the same frequency. The magnitude of the vibration amplitude can be used to estimate the magnitude of the local piezoelectric coefficient. As shown in Figure 10(a), several obvious bright areas (high deflection amplitude) can be seen in the figure, which are considered piezoelectric-active areas. From the 3D amplitude image (Figure 10(b)), more obvious deflection amplitude peaks can be observed more intuitively. However, the distribution of each peak in the tested area is not uniform, which may be due to the uneven dispersion of nanoparticles in the composite films, resulting in higher piezoelectric response in local areas. Combining the two images, it is confirmed that the voltage output of the prepared films in this article is generated from the piezoelectricity.

3.3 Piezoelectric properties of PVDF-HFP/CB/Ni composite films

Figure 11 shows the open-circuit voltage and the effective voltage of the composite films (the vibration amplitude of the plate end is close to 1 mm). Notably, the piezoelectric performance of PVDF-HFP/Ni and PVDF-HFP/CB composite films exceeds that of pure PVDF-HFP films. However, there were slight variations in the thickness of the films and the

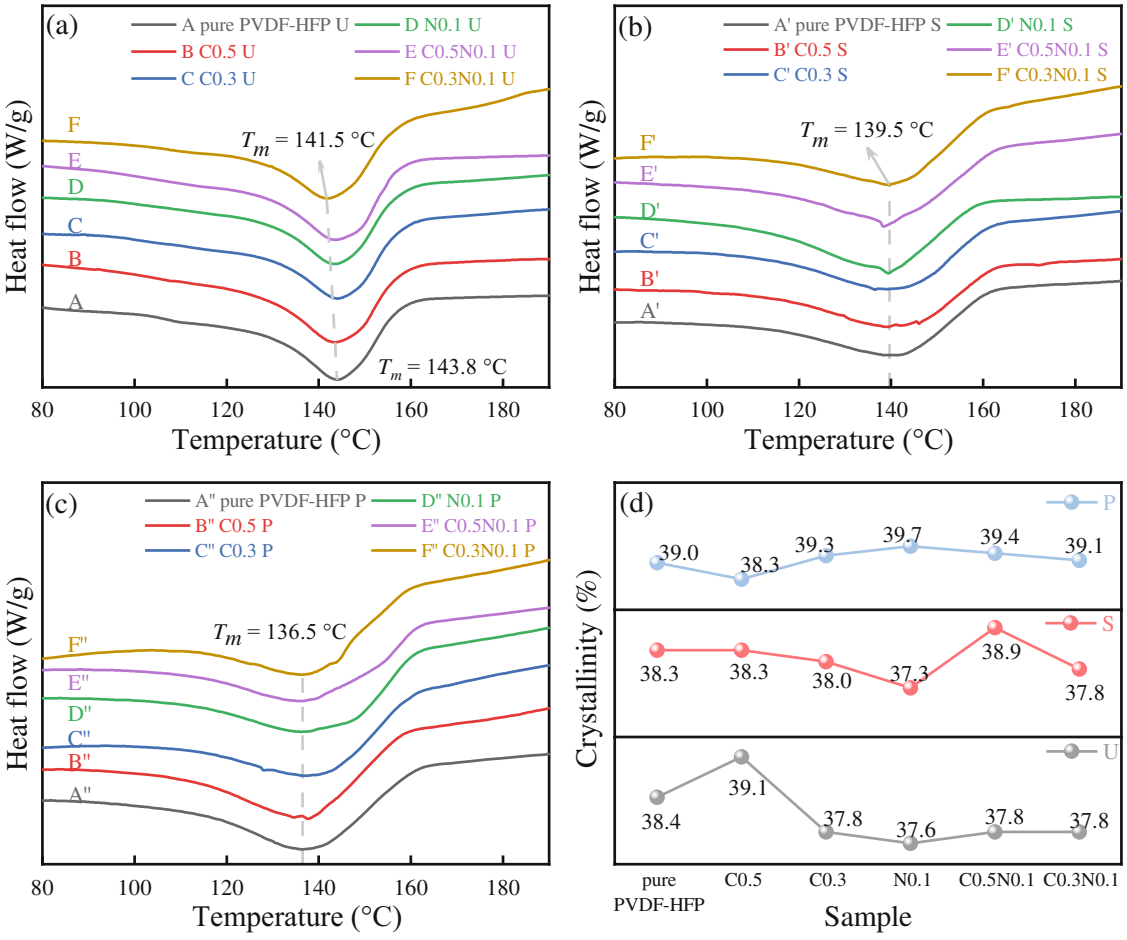

Figure 9: DSC thermograms of PVDF-HFP/CB/Ni composite films: (a) unstretched films (U), (b) stretched films (S), and (c) stretched and polarized films (P). (d) Crystallinity degree of PVDF-HFP/CB/Ni composite films at each stage.

vibration amplitude of the plate end during the experiments. To further investigate the impact of nanofillers on the piezoelectric properties of PVDF-HFP, the calibrated open-circuit voltage was calculated as follows:

$$V_c = V\frac{u_0 t_0}{ut}, \tag{3}$$

where u is the vibration amplitude of the plate end, t is the piezoelectric film thickness, u_0 = 1 mm is the standard

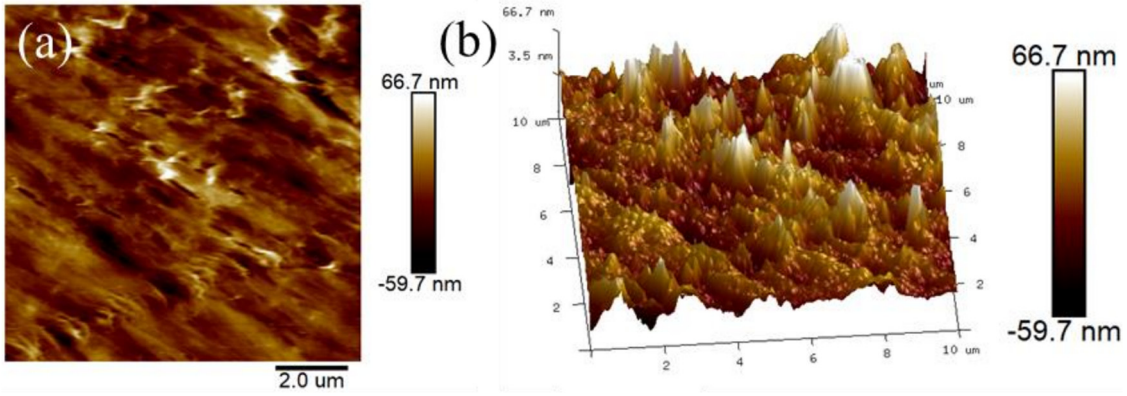

Figure 10: PFM images of PVDF-HFP/CB/Ni composite films: (a) 2D amplitude and (b) 3D amplitude.

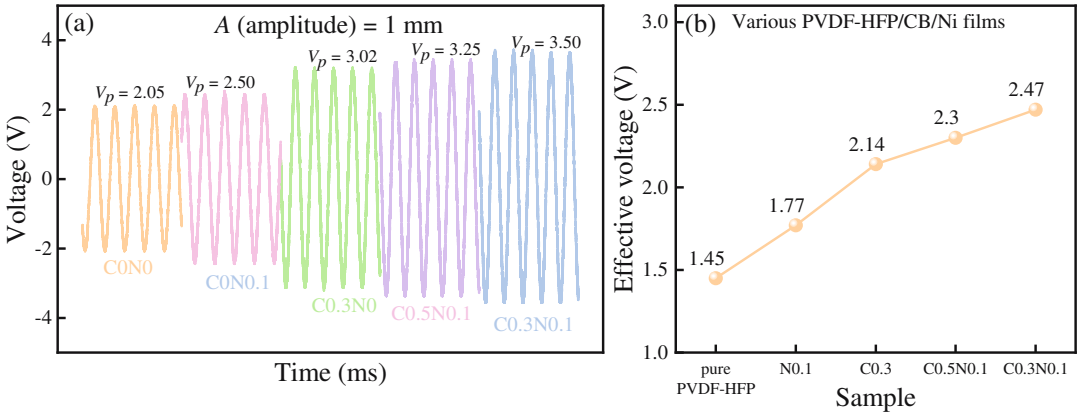

Figure 11: (a) The output voltage of PVDF-HFP/CB/Ni composite films containing different nanofillers. (b) The effective voltage of PVDF-HFP/CB/Ni composite films containing different nanofillers.

vibration amplitude, and t_0 = 100 μm is the standard film thickness. The calibrated open-circuit voltage for the composite film is shown in Figure 12.

Figure 12(a) shows the calibrated open-circuit voltage of pure PVDF-HFP piezoelectric films under different maximum polarized electric fields E_{max}. Notably, when E_{max} =

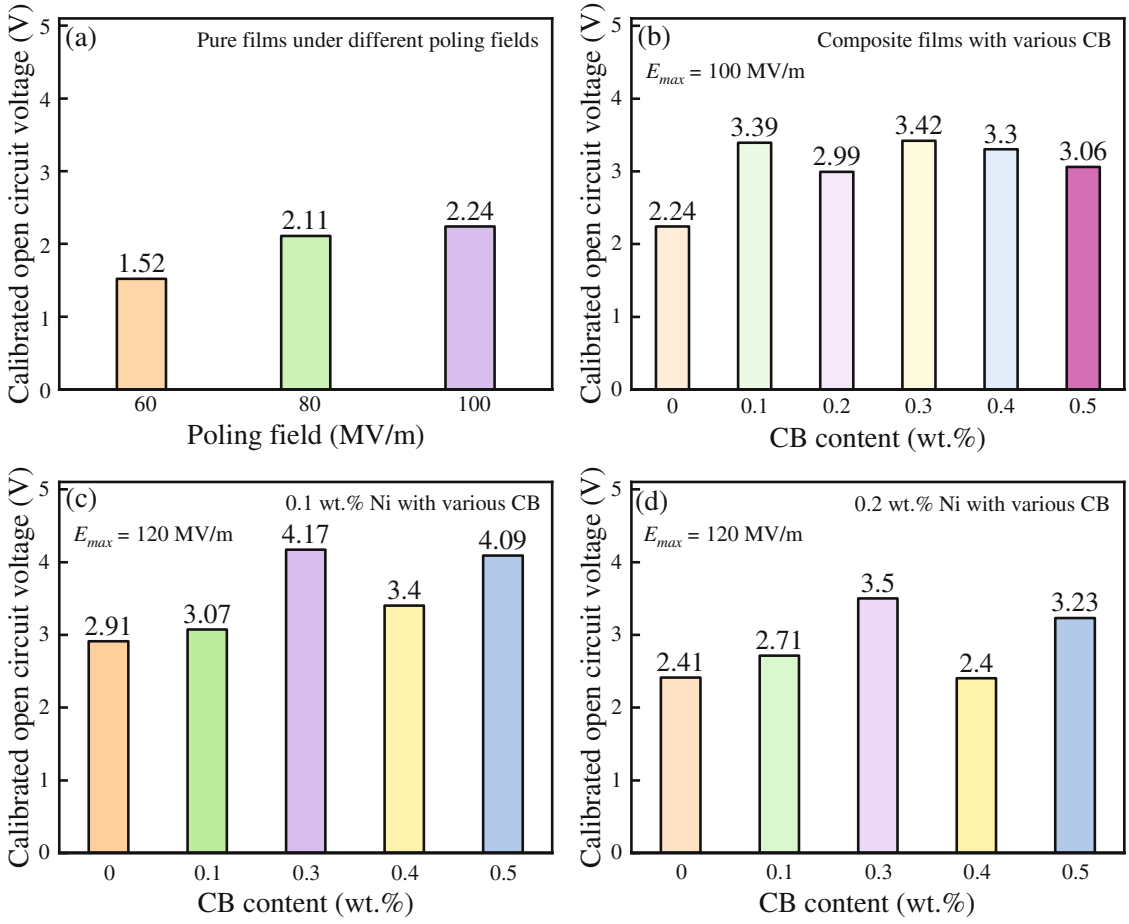

Figure 12: The calibrated open-circuit output voltage of PVDF-HFP/CB/Ni films: (a) neat PVDF-HFP films under different poling electric fields; (b) PVDF-HFP/CB/Ni composites with various CB loadings; (c) PVDF-HFP/CB/Ni composites with 0.1 wt% Ni nanoparticles and various CB loadings; and (d) PVDF-HFP/CB/Ni composites with 0.2 wt% Ni nanoparticles and various CB loadings.

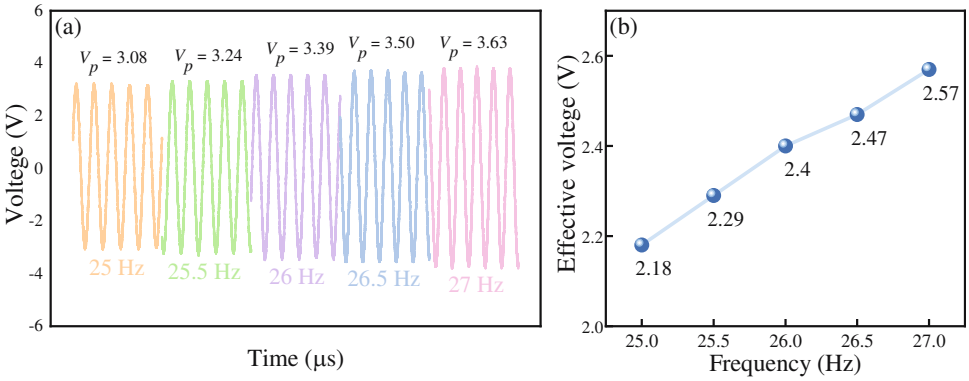

Figure 13: (a) The open-circuit voltage of PVDF-HFP/CB0.3N0.1 composite films vibrated at different frequencies. (b) The effective voltage of PVDF-HFP/CB0.3N0.1 composite films.

100 MV·m^{-1}, the calibrated open-circuit voltage increased to 2.24 V, highlighting the decisive effect of poling on piezoelectric performance. A high poling electric field induces a high degree of internal dipole moment orientation of the polymer along the direction of the electric field (*i.e.*, perpendicular to the surface of the film), thereby improving the voltage generation capability. Studies have shown that the dipole moment of the initial crystallization film is randomly distributed within the matrix, resulting in mutual offset and an overall lack of piezoelectricity [54,55]. For PVDF-HFP/CB composite films, as shown in Figure 12(b), the maximum V_c is 3.42 V (0.3 wt% CB, E_{max} = 100 MV·m^{-1}). For PVDF-HFP/Ni composite films, it is only 2.91 V (0.1 wt% Ni, E_{max} = 120 MV·m^{-1}). Figure 12(c) and (d) shows the V_c of the PVDF-HFP/CB/Ni composite films. It is found that V_c can reach a much higher value when the hybrid nanofillers are added (C0.3 + N0.1:4.17 V; C0.5 + N0.1:4.09 V). From Figure 12, it is found that the increment of the Ni nanofiller content has a negative effect on the piezoelectric performance, which may be caused by the poor dispersion of magnetic nanoparticles. Generally speaking, the piezoelectricity depends on the fraction of the polar β-phase and the orientation of its dipole moments. The addition of conductive CB can form a conductive pathway in the matrix, which can generate stronger interfacial polarization during the poling process to improve the polarization and the degree of dipole moment orientation. However, it also reduces its breakdown electric field strength. In the composite film of PVDF-HFP/CB, the maximum poling electric field is 100 MV·m^{-1}. Under this electric field, the calibrated open-circuit voltage reaches a maximum of 3.5 V. In the experiment, we found that the breakdown failure rate of the film with only CB added is too high. The main reason is that the CB agglomeration area forms an uneven local electric field under the action of the electric field, making it easier to break down. It has been reported that under an external electric field, Ni nanoparticles are prone to form Coulomb islands, which can induce the Coulomb blockade effect and increase the breakdown electric field strength of composite materials, so a higher poling electric field can be applied to improve piezoelectricity [56]. Therefore, the composite film with mixed fillers exhibits a higher breakdown electric field strength and lower breakdown failure rate.

We investigated the open-circuit voltage of PVDF-HFP/C0.3N0.1 composite films near the first-order frequency of the plate by adjusting the vibration frequency of the measurement plate, as shown in Figure 13. The film exhibited varying output voltages as the vibration frequency changed. The highest effective voltage of 2.57 V was observed at a frequency f of 27 Hz. Notably, at a frequency f of 26.5 Hz, which corresponds to the first-order resonance frequency, the measurement plate attained the maximum vibration amplitude under the same excitation voltage.

3.4 Piezoelectric enhancement mechanism

Hybrid fillers play a nucleation role in the initial crystallization stage, which can effectively promote the formation of the β-phase. In the tensile stage, stress concentration occurs at the interface between the nanofillers and the matrix, which induces the transformation of the α-phase to the β-phase. In the process of poling, Ni nanoparticles improve the breakdown electric field strength of the film. It has been reported that under an external electric field, Ni nanoparticles are prone to form Coulomb islands, which can induce the Coulomb blockade effect and improve the breakdown electric field strength of the composite materials, facilitating the polarization of the films under high electric fields. However, CB nanofillers form a conductive network in the composites, and a larger local electric field is

formed near the nanofillers due to the micro-capacitor effect, resulting in stronger interfacial polarization to improve the polarization. As a result, the synergistic effect of the hybrid fillers leads to a higher voltage output.

4 Conclusions

This study uses a solution casting method to prepare PVDF-HFP piezoelectric composite films with high β-phase content and excellent piezoelectric performance. The effects of added nanofillers are discussed in detail. The results show that in the output voltage measurement, the PVDF-HFP/C0.3N0.1 (E_{max} = 120 MV·m^{-1}) composite film exhibits a calibrated open-circuit voltage of 4.17 V, which is 86% higher than that of pure PVDF-HFP films (E_{max} = 100 MV·m^{-1}, 2.24 V), 43% higher than that of PVDF-HFP/Ni(0.1) composite films (2.91 V), and 22% higher than that of PVDF-HFP/CB (0.3) (E_{max} = 100 MV·m^{-1}, 3.42 V) composite films.

Acknowledgments: This work was financially supported by the National Natural Science Foundation of China (No. 51703015) and Fundamental Research Funds for the Central Universities (No. 2020CDJQY-A008).

Funding information: This work was financially supported by the National Natural Science Foundation of China (No. 51703015) and Fundamental Research Funds for the Central Universities (No. 2020CDJQY-A008).

Author contributions: Yang Wang: experiments, writing and editing; Dan Lei: writing and editing; Liangke Wu: funding acquisition, writing-review and editing; Ning Hu: funding acquisition and writing; Huiming Ning, Alamusi, and Yaolu Liu: technical support. All authors have accepted responsibility for the entire content of this manuscript and approved its submission.

Conflict of interest: The authors state no conflict of interest.

References

[1] Zhang, Y., M. Xie, V. Adamaki, and H. K. R. Bowen. Control of electro-chemical processes using energy harvesting materials and devices. *Chemical Society Reviews*, Vol. 46, No. 24, 2017, pp. 7757–7786.

[2] Guo, S., X. Duan, M. Xie, K. C. Aw, and Q. Xue. Composites, fabrication and application of polyvinylidene fluoride for flexible electromechanical devices: A Review. *Micromachines*, Vol. 11, No. 12, 2020, id. 1076.

[3] Mokhtari, F., G. M. Spinks, C. Fay, Z. Cheng, R. Raad, J. Xi, et al. Wearable electronic textiles from nanostructured piezoelectric fibers. *Advanced Materials Technologies*, Vol. 5, 2020, id. 1900900.

[4] Mokhtari, F., G. M. Spinks, S. Sayyar, Z. X. Cheng, A. Ruhparwar, and J. Foroughi. Highly stretchable self-powered wearable electrical energy generator and sensors. *Advanced Materials Technologies*, Vol. 6, 2021, id. 2000841.

[5] Li, M., H. J. Wondergem, M. Spijkman, K. Asadi, I. Katsouras, P. W. Blom, et al. Revisiting the delta-phase of poly(vinylidene fluoride) for solution-processed ferroelectric thin films. *Nature Materials*, Vol. 12, No. 5, 2013, pp. 433–438.

[6] Jin, L., S. Ma, W. Deng, C. Yan, T. Yang, X. Chu, et al. Polarization-free high-crystallization ss-PVDF piezoelectric nanogenerator toward self-powered 3D acceleration sensor. *Nano Energy*, Vol. 50, 2018, pp. 632–638.

[7] Khan, F., T. Kowalchik, and S. R. Warren. Stretching-induced phase transitions in barium titanate-poly(vinylidene fluoride) flexible composite piezoelectric films. *Scripta Materialia*, Vol. 193, 2021, pp. 64–70.

[8] Mishra, S., R. Sahoo, L. Unnikrishnan, A. Ramadoss, and S. M. K. Nayak. Investigation of the electroactive phase content and dielectric behaviour of mechanically stretched PVDF-GO and PVDF-rGO composites. *Materials Research Bulletin*, Vol. 124, 2020, id. 110732.

[9] Mahdi, R. I., W. C. Gan, and W. H. Abd Majid. Hot plate annealing at a low temperature of a thin ferroelectric P(VDF-TrFE) film with an improved crystalline structure for sensors and actuators. *Sensors*, Vol. 14, No. 10, 2014, pp. 19115–19127.

[10] Lei, D., N. Hu, L. Wu, R. Huang, A. Lee, Z. Jin, et al. Preparation of efficient piezoelectric PVDF-HFP/Ni composite films by high electric field poling. *Nanotechnology Reviews*, Vol. 11, No. 1, 2022, pp. 452–462.

[11] Salimi, A. and A. A. Yousefi. Analysis method: FTIR studies of β-phase crystal formation in stretched PVDF films. *Polymer Testing*, Vol. 22, No. 6, 2003, pp. 699–704.

[12] Sabira, K., P. Saheeda, M. C. Divyasree, and S. Jayalekshmi. Impressive nonlinear optical response exhibited by poly(vinylidene fluoride) (PVDF)/reduced graphene oxide (RGO) nanocomposite films. *Optics and Laser Technology*, Vol. 97, 2017, pp. 77–83.

[13] Fakhri, P., H. Mahmood, and B. J. Pegoretti. Improved electroactive phase content and dielectric properties of flexible PVDF nanocomposite films filled with Au- and Cu-doped graphene oxide hybrid nanofiller. *Synthetic Metals*, Vol. 220, 2016, pp. 653–660.

[14] Hu, X., Z. Ding, L. Fei, Y. Xiang, and Y. Lin. Wearable piezoelectric nanogenerators based on reduced graphene oxide and in situ polarization-enhanced PVDF-TrFE films. *Journal of Materials Science*, Vol. 54, No. 8, 2019, pp. 6401–6409.

[15] Wu, C. and M. H. Chou. Polymorphism, piezoelectricity and sound absorption of electrospun PVDF membranes with and without carbon nanotubes. *Composites Science and Technology*, Vol. 127, 2016, pp. 127–133.

[16] Davand, R. and M. Frounchi. Composites of carbon nanotubes with the blend of poly(vinylidene fluoride)/poly(vinyl acetate). *Polymer-Korea*, Vol. 40, No. 2, 2016, pp. 232–237.

[17] Wu, L., W. Yuan, N. Hu, Z. Wang, C. Chen, J. Qiu, et al. Improved piezoelectricity of PVDF-HFP/carbon black composite films. *Journal of Physics D-Applied Physics*, Vol. 47, No. 13, 2014, id. 135303.

[18] Wu, L., M. Jing, Y. Liu, H. Ning, X. Liu, S. Liu, et al. Power generation by PVDF-TrFE/graphene nanocomposite films. *Composites Part B-Engineering*, Vol. 164, 2019, pp. 703–709.

[19] Gan, W. C. and W. H. A. Majid. Effect of TiO_2 on enhanced pyroelectric activity of PVDF composite. *Smart Materials and Structures*, Vol. 23, No. 4, 2014, id. 045026.
[20] Ponnamma, D., A. Erturk, H. Parangusan, K. Deshmukh, M. B. Ahamed, and M. A. Ali Al-Maadeed. Stretchable quaternary phasic PVDF-HFP nanocomposite films containing graphene-titania-$SrTiO_3$ for mechanical energy harvesting. *Emergent Materials*, Vol. 1, No. 1–2, 2018, pp. 55–65.
[21] Yue, L., G. Pircheraghi, S. A. MonemianIca, and M. Z. Ica. Epoxy composites with carbon nanotubes and graphene nanoplatelets – Dispersion and synergy effects. *Carbon*, Vol. 78, 2014, pp. 268–278.
[22] Ma, P., N. A. Siddiqui, G. Marom, and J. Kim. Dispersion and functionalization of carbon nanotubes for polymer-based nanocomposites: A review. *Composites Part a-Applied Science and Manufacturing*, Vol. 41, No. 10, 2010, pp. 1345–1367.
[23] Yang, L., Q. Zhao, Y. Hou, R. Sun, M. Cheng, M. Shen, et al. High breakdown strength and outstanding piezoelectric performance in flexible PVDF based percolative nanocomposites through the synergistic effect of topological-structure and composition modulations. *Composites Part a-Applied Science and Manufacturing*, Vol. 114, 2018, pp. 13–20.
[24] Yang, L., M. Cheng, W. Lyu, M. Shen, J. Qiu, H. Ji, et al. Tunable piezoelectric performance of flexible PVDF based nanocomposites from MWCNTs/graphene/MnO_2 three-dimensional architectures under low poling electric fields. *Composites Part a-Applied Science and Manufacturing*, Vol. 107, 2018, pp. 536–544.
[25] Wu, L., W. Yuan, T. Nakamura, S. Atobe, N. Hu, H. Fukunaga, et al. Enhancement of PVDF's piezoelectricity by VGCF and MWNT. *Advanced Composite Materials*, Vol. 22, No. 1, 2013, pp. 49–63.
[26] Al-Saygh, A., D. Ponnamma, M. A. AlMaadeed, P. P. Vijayan, A. Karim, and M. K. Hassan. Flexible pressure sensor based on PVDF nanocomposites containing reduced graphene oxide- Titania hybrid nanolayers. *Polymers*, Vol. 9, No. 2, 2017, id. 33.
[27] Chen, H., S. Han, C. Liu, Z. Luo, H. D. Shieh, R. Hsiao, et al. Investigation of PVDF-TrFE composite with nanofillers for sensitivity improvement. *Sensors and Actuators a-Physical*, Vol. 245, 2016, pp. 135–139.
[28] Song, S., Z. Zheng, Y. Bi, X. Lv, and S. Sun. Improving the electroactive phase, thermal and dielectric properties of PVDF/graphene oxide composites by using methyl methacrylate-*co*-glycidyl methacrylate copolymers as compatibilizer. *Journal of Materials Science*, Vol. 54, No. 5, 2019, pp. 3832–3846.
[29] Cai, J., N. Hu, L. Wu, Y. Liu, Y. Li, H. Ning, et al. Preparing carbon black/graphene/PVDF-HFP hybrid composite films of high piezoelectricity for energy harvesting technology. *Composites Part a-Applied Science and Manufacturing*, Vol. 121, 2019, pp. 223–231.
[30] Khalifa, M., S. Peravali, S. Varsha, and S. Anandhan. Piezoelectric energy harvesting using flexible self-poled electroactive nanofabrics based on PVDF/ZnO-decorated SWCNT nanocomposites. *JOM*, Vol. 74, No. 8, 2022, pp. 3162–3171.
[31] Sinha, T. K., S. K. Ghosh, R. Maiti, S. Jana, B. Adhikari, D. Mandal, et al. Graphene-silver-induced self-polarized PVDF-based flexible plasmonic nanogenerator toward the realization for new class of self powered optical sensor. *ACS Applied Materials & Interfaces*, Vol. 8, No. 24, 2016, pp. 14986–14993.
[32] Moezzi, M. D., M. Karrabi, and Y. Jahani. Influence of adding carbon black on electrical conductivity in dynamically vulcanized of poly (vinylidene fluoride)/fluoroelastomer composites. *International Journal of Plastics Technology*, Vol. 23, No. 1, 2019, pp. 46–55.
[33] Ke, K., P. Poetschke, N. Wiegand, B. Krause, and B. Voit. Tuning the network structure in poly(vinylidene fluoride)/carbon nanotube nanocomposites using carbon black: Toward improvements of conductivity and piezoresistive sensitivity. *ACS Applied Materials & Interfaces*, Vol. 8, No. 22, 2016, pp. 14190–14199.
[34] Li, T., W. Zhou, Y. Li, D. Cao, Y. Wang, G. Cao, et al. Synergy improvement of dielectric properties and thermal conductivity in PVDF composites with core-shell structured Ni@SiO_2. *Journal of Materials Science-Materials in Electronics*, Vol. 32, No. 4, 2021, pp. 4076–4089.
[35] Senthilkumar, N., K. J. Babu, G. G. Kumar, A. R. Kim, and D. J. Yoo. Flexible electrospun PVdF-HFP/Ni/Co membranes for efficient and highly selective enzyme free glucose detection. *Industrial & Engineering Chemistry Research*, Vol. 53, No. 25, 2014, pp. 10347–10357.
[36] Wu, L., Alamusi, J. Xue, T. Itoi, N. Hu, Y. Li, et al. Improved energy harvesting capability of poly(vinylidene fluoride) films modified by reduced graphene oxide. *Journal of Intelligent Material Systems and Structures*, Vol. 25, No. 14, 2014, pp. 1813–1824.
[37] Wu, L., G. Huang, N. Hu, S. Fu, J. Qiu, Z. Wang, et al. Improvement of the piezoelectric properties of PVDF-HFP using AgNWs. *Rsc Advances*, Vol. 4, No. 68, 2014, pp. 35896–35903.
[38] Karan, S. K., R. Bera, S. Paria, A. K. Das, S. Maiti, and A. Maitra. An approach to design highly durable piezoelectric nanogenerator based on self-poled PVDF/AlO-rGO flexible nanocomposite with high power density and energy conversion efficiency. *Advanced Energy Materials*, Vol. 6, 2016, id. 1601016.
[39] He, L., J. Lu, C. Han, X. Liu, J. Liu, and C. Zhang. Electrohydrodynamic pulling consolidated high-efficiency 3D printing to architect unusual self-polarized β-PVDF arrays for advanced piezoelectric sensing. *Small*, Vol. 18, 2022, id. 2200114.
[40] Yang, J., Y. Zhang, Y. Li, Z. Wang, W. Wang, Q. An, et al. Piezoelectric nanogenerators based on graphene oxide/PVDF electrospun nanofiber with enhanced performances by in-situ reduction. *Materials Today Communications*, Vol. 26, 2021, id. 101629.
[41] Xue, Y., T. Yang, Y. Zheng, K. Wang, E. Wang, H. Wang, et al. Heterojunction engineering enhanced self-polarizaiton of PVDF/$CsPbBr_3$/Ti_3C_2Tx composite fiber for ultra-high voltage piezoelectric nanogenerator. *Advanced Science*, Vol. 10, 2023, id. 2300650.
[42] Ponnamma, D., O. Aljarod, and H. Parangusan. Reduction in piezoelectric voltage generation for the cerium doped nickel ferrite nanoparticles filled with PVDF-HFP nanocomposite. *Results in Physics*, Vol. 13, 2019, id. 102130.
[43] Singh, H. D., S. Singh, and N. Khare. Design of flexible PVDF/$NaNbO_3$/RGO nanogenerator and understanding the role of nanofillers in the output voltage signal. *Composites Science and Technology*, Vol. 149, 2017, pp. 127–133.
[44] Yi, Y., Y. Song, S. Zhang, Z. Cao, C. Li, and C. Xiong. Corona-poled porous electrospun films of Gram-scale Y-doped ZnO and PVDF composites for piezoelectric nanogenerators. *Polymers*, Vol. 14, id. 3912.
[45] Mahadeva, S., J. Berring, K. Walus, and B. Stoeber. Effect of poling time and grid voltage on phase transition and piezoelectricity of poly(vinylidene fluoride) thin films using corona poling. *Journal of Physics D-Applied Physics*, Vol. 46, No. 28, 2013, id. 285305.
[46] Lee, C. and J. Tarbutton. Electric poling-assisted additive manufacturing process for PVDF polymer-based piezoelectric device applications. *Smart materials and structures*, Vol. 23, No. 9, 2014, id. 095044.
[47] Li, L., M. Zhang, M. Rong, and W. Ruan. Studies on the transformation process of PVDF from alpha to beta phase by stretching. *Rsc Advances*, Vol. 4, No. 8, 2014, pp. 3938–3943.

[48] Lanceros-Mendez, S., J. F. Mano, A. M. Costa, and V. H. Schmidt. FTIR and DSC studies of mechanically deformed beta-PVDF films. *Journal of Macromolecular Science-Physics*, Vol. B40, No. 3–4, 2001, pp. 517–527.

[49] Tong, W., Y. Zhang, L. Yu, X. Luan, Q. An, Q. Zhang, et al. Novel method for the fabrication of flexible film with oriented arrays of graphene in poly(vinylidene fluoride-*co*-hexafluoropropylene) with low dielectric loss. *Journal of Physical Chemistry C*, Vol. 118, No. 20, 2014, pp. 10567–10573.

[50] Sencadas, V., R. Jr Gregorio, and S. Lanceros-Mendez. alpha to beta phase transformation and microestructural changes of PVDF films induced by uniaxial stretch. *Journal of Macromolecular Science Part B-Physics*, Vol. 48, No. 3, 2009, pp. 514–525.

[51] Mishra, S., L. Unnikrishnan, S. Nayak, and S. Mohanty. Advances in piezoelectric polymer composites for energy harvesting applications: a systematic review. *Macromolecular Materials and Engineering*, Vol. 304, No. 1, id. 1800463.

[52] Wang, W., H. Fan, and Y. Ye. Effect of electric field on the structure and piezoelectric properties of poly(vinylidene fluoride) studied by density functional theory. *Polymer*, Vol. 51, No. 15, 2010, pp. 3575–3581.

[53] Wu, L., Z. Jin, Y. Liu, H. Ning, X. Liu, Alamusi, et al. Recent advances in the preparation of PVDF-based piezoelectric materials. *Nanotechnology Reviews*, Vol. 11, No. 1, 2022, pp. 1386–1407.

[54] Furukawa, T. Ferroelectric properties of vinylidene fluoride copolymers. *Phase Transitions: A Multinational Journal*, Vol. 18, 2006, pp. 143–211.

[55] Garain, S., S. Jana, T. K. Sinha, and D. Mandal. Design of in situ poled Ce3+ -doped electrospun PVDF/graphene composite nanofibers for fabrication of nanopressure sensor and ultrasensitive acoustic nanogenerator. *ACS Applied Materials & Interfaces*, Vol. 8, No. 7, 2016, pp. 4532–4540.

[56] Zheng, H., X. Liu, X. Dou, and J. Chen. Effect of employing Ni and Ag nanoparticles as third phase on dielectric breakdown strength of $BaTiO_3$/PVDF composites. *Acta Materials Composite Sinica*, Vol. 31, No. 1, 2014, pp. 146–151.